9482 *Biochemistry* **2009,** *48,* 9482–9491
DOI: 10.1021/bi901035j

BIOCHEMISTRY
including biophysical chemistry & molecular biology
Article

Chloroquine Transport in *Plasmodium falciparum*. 2. Analysis of PfCRT-Mediated Drug Transport Using Proteoliposomes and a Fluorescent Chloroquine Probe[†]

Michelle F. Paguio,[‡] Mynthia Cabrera,[‡] and Paul D. Roepe*[,‡,§,∥]

[‡]*Department of Chemistry and* [§]*Department of Biochemistry and Cellular and Molecular Biology and* [∥]*Center for Infectious Diseases, Georgetown University, 37th and O Streets, NW, Washington, D.C. 20057*

Received June 18, 2009; Revised Manuscript Received September 1, 2009

ABSTRACT: Mutations in the PfCRT protein cause chloroquine resistance (CQR), and earlier studies from our laboratory using plasma membrane inside-out vesicles (ISOV) prepared from yeast expressing recombinant PfCRT [Zhang, H., *et al.* (2004) *Biochemistry 43*, 8290−8296] suggested that the putative transporter mediates downhill facilitated diffusion of charged chloroquine (CQ). However, more recent experiments with a fluorescent CQ probe (NBD-CQ) presented in the accompanying paper (DOI 10.1021/bi901034r) indicated that the CQR phenotype in live parasites is associated with a reduced rate of ATP-dependent CQ uptake into the digestive vacuole (DV). An altered rate constant for uptake has multiple interpretations. To further investigate this phenomenon, PfCRT proteins found in chloroquine-sensitive (CQS) and CQR strains of *Plasmodium falciparum* were purified from yeast engineered to express "yeast optimized" *pfcrt* genes, reconstituted into proteoliposomes (PL), and efflux of NBD-CQ was measured from these PL. A membrane-impermeant quencher was used to distinguish intra-PL NBD-CQ from extra-PL NBD-CQ vs time as well as resolve initial rates and rate constants for efflux. Efflux was investigated at a range of NBD-CQ concentrations, in the presence vs absence of pH gradients (ΔpH) and transmembrane potentials (ΔΨ). Explicit turnover numbers for apparent PfCRT-mediated transport were then calculated under these conditions. Our data are consistent with a model wherein PfCRT catalyzes electrochemically downhill diffusion of NBD-CQ out of the DV, in response to ΔΨ or ΔpH, at a rate that can partially compete with the ATP-dependent uptake of NBD-CQ by CQS parasites described in the previous paper. These data allow us to propose a refined model for altered CQ accumulation in CQR malarial parasites.

For more than 20 years the molecular mechanism whereby chloroquine-resistant (CQR)[1] malarial parasites accumulate lower levels of intracellular chloroquine (CQ) in a given time relative to CQ sensitive (CQS) has remained elusive (*1*). A variety of cell biological explanations have been invoked including reduced active accumulation, reduced intracellular binding site capacity, reduced binding site affinity, and various permutations of net outward directed drug transport (e.g., facilitated diffusion, active pumping, or exchange) that compete with passive influx. With the identification of *Plasmodium falciparum* chloroquine-resistant transporter (PfCRT) mutations as the chief CQR *P. falciparum* determinant (*2*, *3*) as well as recent transfection studies that suggest *P. falciparum* multidrug resistant 1 (PfMDR1) protein only modulates PfCRT-mediated resistance (*4*−*6*), more specific molecular hypotheses have been offered. These include that PfCRT mediates downhill diffusion of charged CQ (*7*) or CQ exchange (*8*) and that PfMDR1 mediates adenosine 5′-triphosphate (ATP) dependent transport at the digestive vacuole (DV) membrane (*6*). In the accompanying paper (*9*), we show that the rate constant for DV accumulation of a fluorescent CQ analogue (NBD-CQ) is conspicuously reduced for CQR parasites and that this is due to mutation of PfCRT protein to a CQR isoform. This suggests several possibilities for PfCRT function including the following: CQS isoform PfCRT performs ATP-dependent CQ uptake (presumably secondary active transport since PfCRT does not directly hydrolyze ATP) and CQR PfCRT does not, or CQR isoform PfCRT performs outward mediated drug transport at a rate that can compete with ATP-dependent accumulation.

Recently, we have perfected purification and reconstitution of PfCRT-h (PfCRT protein with a C-terminal hexa-His tag) isoforms into proteoliposomes (PL) and have used these to define a CQ binding site via photolabeling with a perfluoroazido CQ derivative (*10*). We have shown that the CQ pharmacophore clearly binds to PfCRT protein and likely has different affinity for isoforms known to confer CQR in *P. falciparum* malaria and that the pharmacophore binding site likely resides near the DV surface of the membrane and proximal to mutations known to cause CQR (*10*). However, the significance of this binding with regard to putative PfCRT-mediated CQ transport remains

[†]Supported by NIH Grants AI045957 and AI052312 to P.D.R.
*To whom correspondence should be addressed. Phone: (202) 687-7300. Fax: (202) 687-6209. E-mail: roepep@georgetown.edu.
[1]Abbreviations: CQR, chloroquine resistant; CQ, chloroquine; CQS, chloroquine sensitive; PfCRT, *Plasmodium falciparum* chloroquine resistance transporter; PfMDR1, *P. falciparum* multidrug resistant 1; ATP, adenosine 5′-triphosphate; DV, digestive vacuole; NBD-CQ, 6-(*N*-(7-nitrobenz-2-oxa-1,3-diazol-4-yl)amino)hexanoic acid (2-{[4-(7-chloroquinolin-4-ylamino)pentyl]ethylamino}ethyl)amide; PfCRT-h, PfCRT protein with a C-terminal hexa-His tag; PL, proteoliposomes; ISOV, inside-out vesicles; $\Delta\mu_{H^+}$, proton electrochemical gradient; ΔΨ, transmembrane potential; YNB w/o a.a., yeast nitrogen base extract without amino acids; oxonol V, bis(3-phenyl-5-oxoisoxazol-4-yl)-pentamethamine oxonol; CM, crude membranes; DTT, dithiothreitol; PIC, protease inhibitor cocktail; BSA, bovine serum albumin; DM, dodecyl β-D-maltoside ; TX-100, Triton X-100; iRBC, infected red blood cells; ΔpH, pH gradient; $\Delta\Psi^-$, negative membrane potential inside; $\Delta\Psi^+$, positive membrane potential inside; VPL, verapamil; MQ, mefloquine.

 Published on Web 09/02/2009

unknown, although several hypotheses have been offered. One popular model is that mutant (CQR associated) PfCRT catalyzes active net outward transport of CQ (presumably as CQ^+ or CQ^{2+}) from the DV. Earlier evidence for PfCRT-mediated transport of CQ included flow dialysis experiments with yeast inside-out vesicles (ISOV) harboring recombinant PfCRT (*7*) as well as fast filtration studies with *Dictyostelium* vesicles harboring recombinant PfCRT (*11*). Data from these two studies are consistent with downhill facilitated diffusion of charged CQ by PfCRT. Other data include some evidence for trans-stimulated counterflow under certain conditions (*8*, *12*). However, this model has been challenged by Bray, Ward, and colleagues (*13*) based on their inability to reproduce counterflow phenomena without special preloading conditions. Bray *et al.* suggested instead that PfCRT may mediate downhill drug efflux in response to a proton electrochemical gradient ($\Delta\mu_{H^+}$), a proposal also suggested earlier via the flow dialysis experiments with yeast plasma membrane ISOV harboring recombinant PfCRT (*7*). A third possibility that has not been discussed as extensively is that PfCRT could be an ion or osmolyte channel (*14*) and that binding of CQ and other quinoline drugs "gates" the function of the channel such that physical−chemical driving forces that govern the passive influx and binding of CQ are altered in a drug-dependent way. Ultimately, distinction between these models and perhaps others depends on kinetic and thermodynamic analysis of drug transport at a resolution that has not been possible until now.

In this paper, we used PL harboring purified PfCRT-h isoforms, yeast ISOV preparations, and the NBD-CQ probe described in the accompanying paper to test whether PfCRT directly transports CQ. Our results are consistent with PfCRT catalyzing transmembrane potential driven facilitated diffusion of charged CQ.

MATERIALS AND METHODS

Materials. Difco yeast nitrogen base extract without amino acids (YNB w/o a.a.) was from BD (Sparks, MD). His GraviTrap gravity-flow columns and Amersham ECL Plus Western blotting detection reagents were from GE Healthcare (Piscataway, NJ). *Escherichia coli* polar lipid extract came from Avanti Polar Lipids, Inc. (Alabaster, AL). Spectra/Por Float-A-Lyzer cellulose membranes were from Spectrum Laboratories, Inc. (Rancho Dominguez, CA). The anti-His HRP conjugate and 6×His protein ladder were purchased from Qiagen (Valencia, CA). Ecoscint A scintillation liquid came from National Diagnostics (Atlanta, GA) while bis(3-phenyl-5-oxoisoxazol-4-yl)pentamethamine oxonol (oxonol V) was from Invitrogen (Carlsbad, CA). All other chemicals were of reagent grade or better and from Sigma (St. Louis, MO).

Preparation of Yeast Crude Membranes. PfCRT-h isoforms were isolated from single colonies of *Pichia pastoris* previously transformed with pPIC3.5/pfcrt-his plasmid DNA (*10*, *15*) that were grown in minimal glycerol medium lacking histidine (1% glycerol, 1.34% YNB w/o a.a., 4×10^{-5} % D-biotin) to exponential phase and then induced with minimum methanol media (0.5% methanol, 1.34% YNB w/o a.a., 4×10^{-5} % D-biotin). Yeast cells were harvested after at least 21 h of induction, and crude membranes (CM) were isolated using the glass bead method (*16*) with a few modifications (*10*, *17*). Briefly, cell pellets were washed three times with harvest buffer (0.1 M glucose, 50 mM imidazole, pH 7.5) and resuspended in breaking buffer (0.1 M glucose, 0.25 M sucrose, 1 mM $MgCl_2$, 50 mM imidazole, pH 7.5) supplemented with 1 mM dithiothreitol (DTT) and protease inhibitor cocktail (PIC) before mechanically lysing them with 0.5 mm glass beads at 4 °C using a BioSpec BeadBeater-type homogenizer (Bartlesville, OK). The homogenate was centrifuged at 1000*g* for 5 min twice and the resulting supernatant at 3000*g* for 15 min. The supernatant from the last spin was finally centrifuged at 100000*g* for 1 h (all centrifugations were done at 4 °C). The pellets were resuspended in suspension buffer (1 mM $MgCl_2$, 10 mM imidazole, pH 7.5) supplemented with PIC and stored at −80 °C. Protein concentrations were quantified using Amido black with bovine serum albumin (BSA) as the standard following trichloroacetic acid precipitation.

Purification and Reconstitution of Recombinant PfCRT. PfCRT-h was purified and reconstituted essentially via the procedures of Howard and Roepe (*17*) with some modifications (*10*). CM harboring PfCRT-h were resuspended in solubilization buffer (0.5% dodecyl β-D-maltoside (DM), 500 mM NaCl, 250 mM sucrose, 20% glycerol, 1 mM $MgCl_2$, 6.5 mM β-mercaptoethanol, 50 mM Tris, pH 7.5, supplemented with PIC) at a protein concentration of 2 mg/mL. After mixing gently for 1 h at 4 °C, the unsolubilized proteins were removed through centrifugation at 100000*g* for 1 h at 4 °C. The solubilized PfCRT-h was purified via immobilized affinity chromatography by loading the supernatant into a His GraviTrap gravity-flow column previously preequilibrated with wash buffer (20 mM imidazole in solubilization buffer). The column was washed twice with wash buffer, and the bound proteins were eluted with elution buffer (500 mM imidazole in solubilization buffer). Eluate was mixed with 1.4% *E. coli* polar lipid and incubated on ice for 30 min before dialyzing them overnight at 4 °C against 900 volumes of dialysis buffer (140 mM sodium or potassium salt, 70 mM sucrose, 4 mM magnesium salt, 1 mM β-mercaptoethanol, 10 mM Mes−Tris, pH 6.5), the pH of which dictates the internal pH of PL, using Float-A-Lyzer regenerated cellulose membranes (molecular mass cutoff = 25 kDa). The dialysis buffer was changed with fresh buffer after 16 h, and dialysis was allowed to continue for another 4 h. The PL were centrifuged at 200000*g* for 1 h at 4 °C, resuspended in fresh dialysis buffer, aliquoted, snap frozen in dry ice−ethanol, and kept at −80 °C until use. Control PL were made in parallel using CM from yeast cells not expressing PfCRT-h (*P. pastoris* transformed with empty pPIC3.5 plasmid); meaning, column fraction that elutes at the same time relative to the PfCRT fraction but that originates from DM solubilized control yeast membranes were used. Protein concentrations were again determined using Amido black with BSA as the standard. Typically, about 2 mg of purified PfCRT-h was derived from 50 mg of CM (4% yield).

Immunodetection of PfCRT-h. Sodium dodecyl sulfate−polyacrylamide gel electrophoresis was performed using 12% resolving Tris-HCl gels. Serial dilutions of 6×His protein ladder were loaded next to PfCRT-h PL samples. Gels were electrophoresed at 110 V for 90 min, and the proteins were transferred to polyvinylidene fluoride membranes through tank-blotting for 16 h at 40 mA and 4 °C. Membranes were immunodetected with Qiagen's anti-His HRP conjugate, and the chemiluminescent reactions were executed using Amersham ECL Plus Western blotting detection reagents following the manufacturers' instructions. Chemiluminescence was captured by Kodak Image Station 2000 mm (Rochester, NY).

Determination of PfCRT-h Content. The number of PfCRT-h molecules per microgram of PL was calculated through densitometry of polyhistidine-detected PfCRT-h (*10*, *18*). Band densities were processed and quantified using ImageJ from NIH

(Bethesda, MD). The linear fit to the protein standards' band density plotted against protein amount and PfCRT-h's predicted molecular mass of 49.5 kDa were then used to calculate for moles of PfCRT-h per microgram of PL.

Calibration of Membrane Potential. PL reconstituted with 140 mM NaCl were first equilibrated with 5 μM oxonol V and 5 μM valinomycin in 3 mL of Mes−Tris, pH 6.5, buffer containing 138.6 mM NaCl and 1.6 mM KCl for 2 min at 37 °C. KCl was then added every 2 min such that final external KCl concentrations were 40, 60, 80, 100, 110, and 120 mM. Fluorescence was monitored by a PTI Alphascan fluorometer (Birmingham, NJ) at excitation wavelength of 602 nm and emission wavelength of 636 nm. The change in fluorescence upon each KCl addition was plotted against Nernst potential. Membrane potential values were calculated using the Nernst equation, $E = (RT/zF)$ ln-$([X_{out}]/[X_{in}])$, where R is the universal gas constant (8.314 J K^{-1} mol^{-1}), T is temperature, z is number of transferred electrons, F is Faraday's constant (9.648 × 10^4 $Cmol^{-1}$), $[X_{out}]$ is external ion concentration, and $[X_{in}]$ is internal ion concentration.

NBD-CQ Efflux Assay. NBD-CQ fluorescence was monitored continuously by a PTI Alphascan fluorometer (Birmingham, NJ) with a water-jacketed cuvette holder which maintained the temperature at 37 °C. Measurements were done at excitation and emission maximum wavelengths of 470 and 550 nm, respectively, at a rate of four points per second.

PL were first preloaded with NBD-CQ for 20 min at 37 °C before diluting them into 3 mL of transport buffer (140 mM sodium or potassium salt, 70 mM sucrose, 4 mM magnesium salt, 1 mM DTT, 10 mM Mes−Tris) in a 4.5 mL methacrylate cuvette. A star-head magnetic stir bar continuously stirring at the bottom of the cuvette ensured rapid mixing of contents. Fluorescence was quenched by the addition of 2 mM sodium dithionite 5 min after PL addition or prior to start of measurement. Finally, 1% Triton X-100 (TX-100) was added to permeabilize membranes. Each experiment was done in triplicate using two independent PL preparations, and standard error means were computed. Turnover numbers were derived from initial rates. Kinetic data were analyzed using SigmaPlot 9.0 from Systat Software, Inc. (San Jose, CA).

^{3}H-CQ Accumulation. ISOV were made from yeast membranes expressing PfCRT via osmotic lysis, homogenization, and separation in a dextran/polyethylene glycol two-phase system (*19*). Fifty micrograms of PfCRT ISOV was mixed with 100 nM ^{3}H-CQ (1 μCi/mmol) in 500 μL of transport buffer (140 mM KCl, 330 mM sucrose, 4 mM $MgCl_2$, 1 mM DTT, 10 mM MES−Tris, pH 8) at room temperature. Samples were incubated for 0, 1, 5, 10, 20, or 40 min in the absence or presence of 2 mM ATP, each done in triplicate. Incubations were stopped with the addition of 2 mL of ice-cold transport buffer. ISOV were filtered by vacuum filtration using a 0.45 mm Whatman GF/F filter, washed twice with the same ice-cold assay buffer, and mixed with 14 mL of Ecoscint A scintillation liquid. Radioactivity was measured using a Beckman LS6500 scintillation counter (Fullerton, CA). For each time point, readings for experiments done in the absence of ATP were subtracted from those done in the presence of the said substrate to remove any nonspecific binding.

RESULTS

As described (*9*), a CQ fluorescent analogue (NBD-CQ) was synthesized via reductive amination of *N-t*-Boc-glycinal with monodesethyl-CQ. Drug susceptibility assays and confocal microscopy

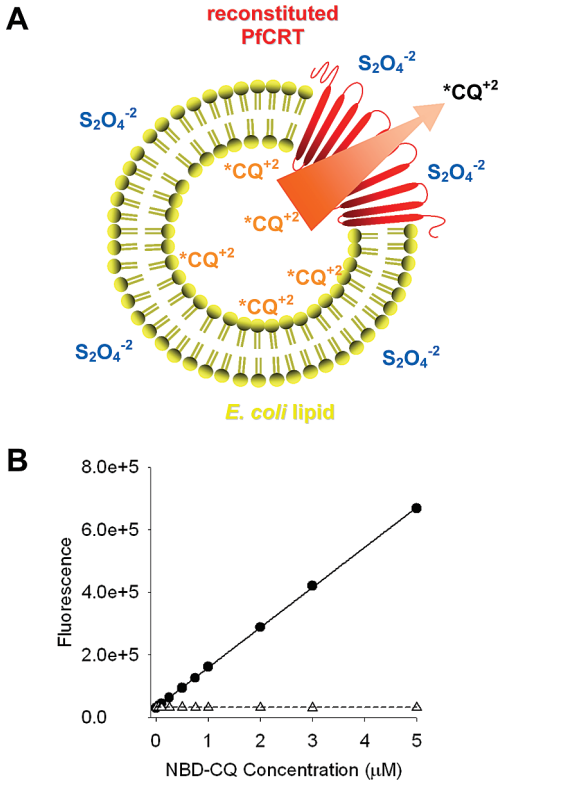

FIGURE 1: (A) Schematic representation of the NBD-CQ efflux assay using reconstituted purified PfCRT. The movement of the CQ probe (asterisk denotes NBD) from the PL via PfCRT (red transmembrane domains) was studied using an extra PL quencher (sodium dithionite, $S_2O_4^{2-}$). (B) The presence of 2 mM sodium dithionite (△) nearly completely quenches fluorescence of NBD-CQ (●) in pH 6.5 Mes−Tris buffer at the range of concentrations used.

revealed that pharmacological activity and subcellular localization of the probe are similar relative to CQ for both CQS and CQR parasites. Thus validated as a suitable tool for CQ transport studies, NBD-CQ influx and efflux kinetics for live infected red blood cells (iRBC) were examined under physiologic conditions. Results were suggestive of PfCRT-mediated drug efflux, but live cell experiments cannot unequivocally distinguish between several molecular models for how decreased CQ accumulation may be due to mutant PfCRT, and precise quantification of any PfCRT-mediated drug efflux is impossible due to the inability to unequivocally quantify altered intra DV binding for CQS vs CQR parasites. In order to directly test how mutant PfCRT may contribute to the altered cellular transport of NBD-CQ for CQR parasites, kinetic NBD-CQ transport assays were developed for PL harboring purified reconstituted PfCRT-h. The use of PL greatly reduces complexities inherent to live cell transport experiments, such as variable heme binding as proposed for CQR malarial parasites by several groups (*9*, *20*, *21*). PL also allow direct examination of the effects of pH gradients (ΔpH) and ΔΨ on drug transport kinetics.

PfCRT-mediated NBD-CQ efflux was assessed using PfCRT-h purified from yeast CM overexpressing the protein. Our procedure for reconstitution of DM-solubilized PfCRT-h through dialysis was previously shown to yield PL with PfCRT-h primarily in an orientation the same as that found for the DV membrane, namely, with N- and C-termini disposed to the outside surface (*10*). We therefore envisioned that preloading these PL with NBD-CQ, followed by injection into a rapidly mixed transport medium harboring an effective NBD quencher such as sodium dithionite ($Na_2S_2O_4$), would allow us to distinguish passive efflux

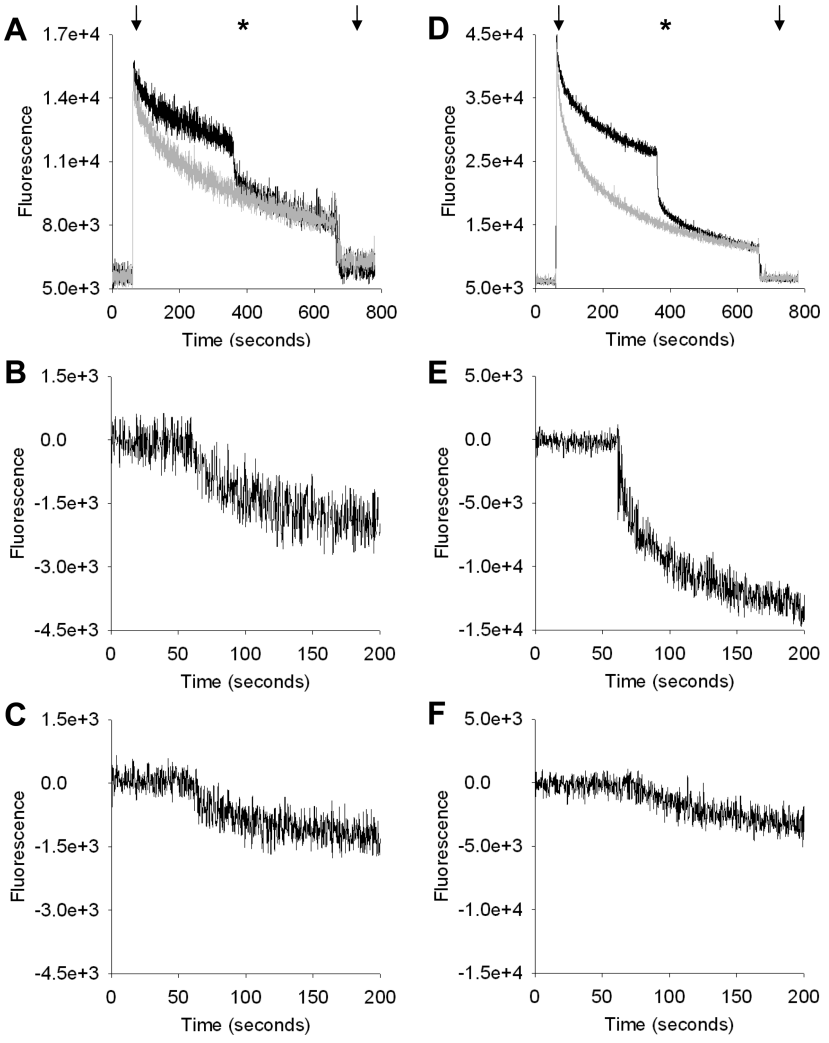

FIGURE 2: Representative raw traces obtained in NBD-CQ efflux assays. (A, D) The first arrow indicates the addition of PfCRT PL preloaded with NBD-CQ for 20 min into the buffer. After 5 min, 2 mM sodium dithionite was added to quench NBD-CQ molecules outside the PL (black traces, asterisk). The second arrow denotes the addition of 1% Triton X-100 which permeabilizes the membranes and immediately quenches remaining fluorescence. The gray trace corresponds to parallel experiments using the same PL preparations, performed with the sodium dithionite already present in the buffer at the start. (B, E) Subtracting the black traces from the gray traces generated difference traces for PfCRT containing PL. (C, F) Executing the same approach using control PL gave control difference traces. Panels A, B, and C correspond to traces obtained from PL preloaded with 1 μM NBD-CQ while panels D, E, and F were from those preloaded with 5 μM NBD-CQ. Panels C−F were shortened to first 200 s to provide a closer view of the kinetics provided by the traces.

from any efflux directly catalyzed by PfCRT. Figure 1A depicts the assay in cartoon form, and Figure 1B confirms that sodium dithionite (△, bottom line) nearly completely quenched NBD-CQ fluorescence measured in its absence, at the relevant range of concentrations (●, top line). Note also that fluorescence vs NBD-CQ concentration was linear over this range, allowing for convenient molar quantification of flux.

Figure 2 shows representative efflux assay data for NBD-CQ-preloaded PL (1 μM probe-loaded PL in Figure 2A−C; 5 μM probe-loaded PL in Figure 2D−F) fast diluted into 3 mL of Mes−Tris buffer that is rapidly mixed by a magnetic stir bar. Due to the hydrophobic weak base character of the probe, these PL contain multiple populations of NBD-CQ, including trapped intraproteoliposomal as well as intramembranous probe. To clearly distinguish actual transmembranous efflux of trapped intraproteoliposomal probe from intramembranous redistribution and other artifacts, two simple experiments were done for each NBD-CQ-preloaded PL preparation. Gray traces in panels A and D show data obtained when the preloaded PL were fast diluted into buffer that already contains sodium dithionite (PL injected at the first arrow), whereas the black traces in the same panels show companion dilutions into the same buffer that did not initially contain dithionite. For the black traces, dithionite was instead rapidly injected at the asterisk. In both experiments, detergent was added at the second arrow to randomize probe throughout the cuvette.

The instantaneous increase in signal (first arrow) upon dilution into buffer without sodium dithionite (black traces, panels A and D) was due to the sudden presence of NBD-CQ-loaded PL. This was followed by a decrease in fluorescence that reflects the sum of multiple changes in environment as NBD-CQ populations move from the acidic PL interior to lipid phase, perhaps between membrane leaflets, or from lipid phase to the aqueous exterior. Additional artifacts are also possible due to rapid mixing of the preloaded PL. Five minutes after injecting the preloaded PL, that portion of NBD-CQ fluorescence that now truly represents extra proteoliposomal, aqueous probe in the mixture was revealed by instantaneous quenching upon addition of sodium dithionite (Figure 2A,D, black traces, asterisk) because the quencher does not cross the PL membrane (*22*). Addition of sodium dithionite at

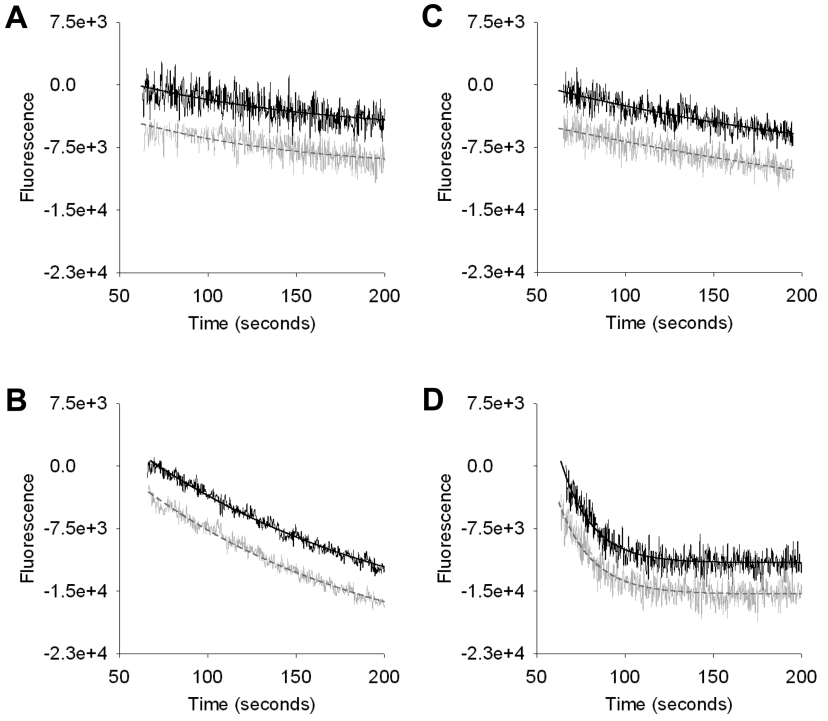

FIGURE 3: Representative control subtracted difference HB3 (black solid lines) and Dd2 (gray dashed lines) efflux traces for experiments (A) without ΔpH and ΔΨ, (B) with a 2 unit ΔpH and without ΔΨ, (C) with $\Delta\Psi^-$ in the absence of ΔpH, and (D) with $\Delta\Psi^+$ in the absence of ΔpH.

progressively shorter time points yielded progressively smaller levels of instantaneous quenching (Figure S1, Supporting Information).

In parallel experiments wherein sodium dithionite was added to the buffer prior to injection of the PL (Figure 2A,D, gray traces), the constant presence of sodium dithionite at the start led to more pronounced, immediate quenching of external NBD-CQ as it exits the PL. Gray and black traces converged at 400 s, showing that the same portion of total NBD-CQ signal that was instantaneously quenched at 5 min (a time wherein we expect the majority of preloaded NBD-CQ to have left the PL) was also quenched vs time as it exits toward the continuous presence of sodium dithionite (Figure 1A,D). Thus, simple subtraction of the companion traces (gray minus black) yielded a difference trace (Figure 2B,E) that removed changes in total NBD-CQ fluorescence that are not unequivocally due to transmembranous movement and that also isolates the kinetic character of NBD-CQ efflux.

Difference traces for control PL (see Methods) preloaded and fast diluted under identical conditions (Figure 2C,F) were subsequently subtracted from those for HB3 PfCRT (CQS isoform) and Dd2 PfCRT (CQR isoform) PL. Multiple traces from at least three replicates for each of at least two independent PL (at least six in total) were then mathematically fitted to determine initial rates and rate constants (see below). Representative PfCRT efflux traces are shown in Figure 3 for HB3 PfCRT (black lines) and Dd2 PfCRT (gray lines) with the single exponential fits superimposed on these traces.

PfCRT-mediated efflux was evaluated under various conditions. When PL prepared at pH 6.5 were diluted into buffer of the same pH, no ΔpH was present and rather slow diffusion of NBD-CQ was noted (Figure 3A). But when the same PL were diluted into pH 7.5 or 8.5 buffer, a ΔpH of 1 or 2 units was established and faster efflux of NBD-CQ was observed for both HB3 and Dd2 PL (Figure 3B, which shows efflux in the presence of a 2 unit ΔpH). To examine the effects of ΔΨ in the absence of a ΔpH, 5 μM valinomycin was added to buffer at the same pH as that used to reconstitute the PL (*17*, *23*). An internal negative membrane potential ($\Delta\Psi^-$) is generated when PL reconstituted with KCl were fast diluted into equimolar NaCl buffer containing valinomycin (Figure 3C), and an internal positive potential ($\Delta\Psi^+$) is generated for PL formed in the presence of NaCl fast diluted into KCl (Figure 3D). Efflux in the presence of $\Delta\Psi^-$ was similar to efflux in the presence of no driving force, whereas $\Delta\Psi^+$ promoted conspicuously faster efflux relative to all other conditions tested.

To test whether all interior NaCl PL samples generated $\Delta\Psi^+$ of similar magnitude, anionic oxonol V assays were used as described (*17*) to empirically calibrate the magnitude of ΔΨ (Figure 4). As shown, PL reconstituted with 140 mM NaCl were diluted into 138.4 mM NaCl/1.6 mM KCl and allowed to equilibrate with 5 μM oxonol V and 5 μM valinomycin to generate low $\Delta\Psi^+$ (Figure 5A, 0−50 s) before adding increasing amounts of KCl (Figure 5A, arrows). Percent change in fluorescence for each addition of KCl was plotted as a function of calculated Nernst potential (Figure 4B). HB3 PfCRT (Figure 4B, ●), Dd2 PfCRT (Figure 4B, gray Δ), and control PL (Figure 4B, □) gave similar fluorescence changes upon these additions of KCl aliquots, indicating that the ΔΨ formed for all samples were comparable in magnitude under these conditions. Hence, any kinetic differences between traces in Figure 3D were not due to differences in the magnitude of ΔΨ.

With known ΔpH, empirically calibrated ΔΨ, and the ability to control intra-PL [NBD-CQ], initial rates and rate constants for NBD-CQ efflux were quantitatively compared for HB3 vs Dd2 PL. Traces were converted to number of NBD-CQ molecules per second using linear molar NBD-CQ fluorescence calibration plots (not shown) and also fitted to a single-exponential decay function, $y = y_0 + ae^{-bx}$. Efflux rate constants for HB3 PfCRT and Dd2 PfCRT PL were nearly superimposable ± ΔpH and ΔΨ (not shown), implying similar efflux is catalyzed by both PfCRT

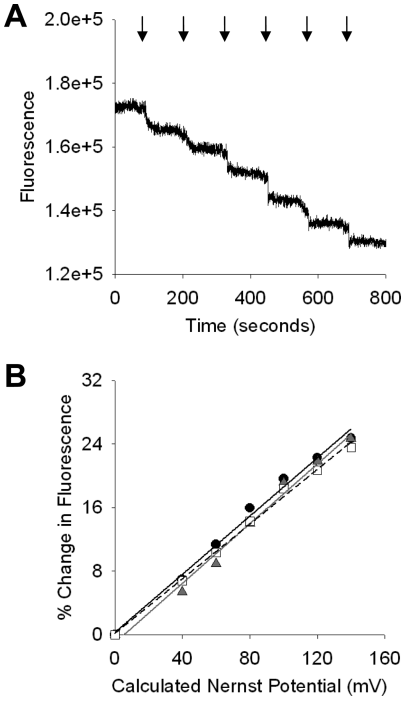

FIGURE 4: Calibration of membrane potential via the anionic dye oxonol V showed no differences between PfCRT PL and control PL in the presence of symmetrical chloride. (A) Control PL reconstituted with 140 mM NaCl were equilibrated with 5 μM oxonol V and 5 μM valinomycin in buffer containing 138.6 mM NaCl and 1.6 mM KCl (0−120 s). Addition of KCl every 2 min resulted in the following final external KCl concentrations: 40 mM (121−240 s, first arrow), 60 mM (241−360 s, second arrow), 80 mM (361−480 s, third arrow), 100 mM (481−600 s, fourth arrow), 110 mM (600−720 s, fifth arrow), and 120 mM (721−840 s, sixth arrow). The experiment was performed three times and repeated for PfCRT PL. (B) The $\Delta\Psi$-driven redistribution of oxonol V in HB3 (●), Dd2 (▲), and control (□) under symmetrical chloride conditions was evaluated by plotting the change in fluorescence as a function of Nernst potential, which were calculated using the Nernst equation, $E = (RT/zF)\ln([X_{out}]/[X_{in}])$.

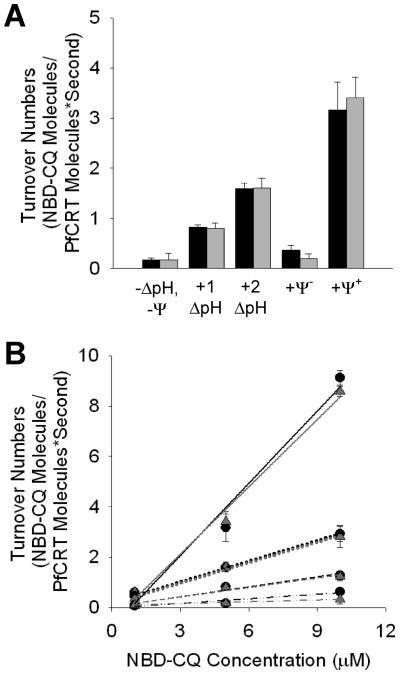

FIGURE 5: PfCRT-mediated NBD-CQ efflux is via facilitated diffusion. (A) HB3 (black bars) and Dd2 (gray bars) PL preloaded with 5 μM NBD-CQ gave similar turnover numbers under different conditions denoted on the x-axis. (B) NBD-CQ efflux in HB3 (●) and Dd2 (▲) PL in the absence (dashed-dotted lines) and presence of a 1 unit (dashed lines) or 2 unit (dotted lines) ΔpH gradient was linear over the range of concentrations used, as well as in the presence of $\Delta\Psi^+$ (solid lines).

isoforms. To quantify any small differences between HB3 and Dd2 PfCRT-mediated efflux, explicit turnover was calculated by dividing the initial rate of efflux (obtained from fitting the first 20 s of NBD-CQ efflux to a linear equation, $y = y_0 + ax$) by the number of PfCRT-h molecules in a given PL preparation, which was calculated via quantitative densitometry as described previously (*10*, *18*).

Figure 5 highlights several important conclusions. First, PfCRT-h PL preloaded with 5 μM NBD-CQ yielded the same turnover number of 0.17 NBD-CQ molecules per PfCRT per second for either HB3 (black bars) or Dd2 (gray bars) when neither a ΔpH nor $\Delta\Psi$ was present across the PL membrane (Figure 5A, left side). Introducing a 1 unit ΔpH increased turnover to 0.83 and 0.80 NBD-CQ/PfCRT/second for HB3 and Dd2 PL, respectively, while a 2 unit ΔpH raised these values further to 1.59 and 1.61 NBD-CQ/PfCRT/second, respectively. Surprisingly, these results suggest that the rate of outward movement of CQ via PfCRT is similar for either CQS or CQR parasites, when the magnitude of DV ΔpH is the same. The data also suggest CQ flux could be either H^+-coupled or electrogenic, since the presence of ΔpH significantly increases turnover. Turnover calculated for PL with $\Delta\Psi^-$ or $\Delta\Psi^+$ (Figure 5A, right side) supports the latter. In the case of a $\Delta\Psi^+$ formed by diluting PL with 140 mM entrapped NaCl into 140 mM KCl with valinomycin (Figure 5A, far right), Dd2 PL reproducibly showed slightly faster efflux relative to HB3 (mean = 3.41 vs 3.27 NBD-CQ/PfCRT/second), but within our resolution, the increase was not statistically significant. Table 1 further summarizes NBD-CQ turnover numbers calculated for PL preloaded with 5 μM NBD-CQ vs various parameters and for an array of control experiments.

Importantly, increases in flux vs NBD-CQ concentration trapped within the PL are linear (Figure 5B). In the absence of any ΔpH or $\Delta\Psi$ (Figure 5B, dashed-dotted lines), NBD-CQ efflux also increased linearly as a function of probe concentration for either HB3 (Figure 5A, ●) or Dd2 PfCRT PL (Figure 5B, gray △). Turnover increased at all NBD-CQ concentrations when a 1 unit ΔpH was introduced (Figure 5B, dashed lines) and increased further when a 2 unit ΔpH was present (Figure 5B, dotted lines). But in both cases, and also in the case of a $\Delta\Psi^+$ (Figure 5B, top lines), increased turnover vs NBD-CQ concentration was linear over the physiologically relevant range of 1−10 μM NBD-CQ.

A key observation made for live cells is that the rate constant for ATP-dependent accumulation of probe was reduced for Dd2 vs HB3 parasites. To examine whether this could be due to HB3 PfCRT-mediated uptake of probe that is lost upon mutation to the Dd2 isoform, we wished to reverse the directionality of our sodium dithionite PL assay (to monitor uptake into the PL). However, we were unable to form good PL by dialysis in the continuous presence of sodium dithionite. ATP-dependent accumulation of ^{3}H-CQ into yeast plasma membrane ISOV harboring PfCRT was therefore measured (*7*, *15*). As expected (*7*), Dd2 ISOV (Figure 6, gray △) showed reduced accumulation relative to control ISOV with no PfCRT (Figure 6, □). Importantly, and again consistent with previous results (*7*), HB3 ISOV (Figure 6, ●) did not show any significantly increased accumulation of ^{3}H-CQ relative to control.

Table 1: NBD-CQ Turnover Numbers of HB3 and Dd2 PfCRT PL

				turnover nos. (NBD-CQ molecules/(PfCRT molecules·s))	
setup[a]	ΔpH_{out}	$\Delta\Psi_{in}$	CQ_{ex} or VPL_{ex}	HB3	Dd2
A				0.17 ± 0.04	0.17 ± 0.13
B	+1			0.83 ± 0.05	0.80 ± 0.11
C	+2			1.59 ± 0.11	1.61 ± 0.18
D		−positive		0.00 ± 0.00	0.00 ± 0.00
E		−negative		0.25 ± 0.06	0.11 ± 0.01
F		+positive		3.27 ± 0.55	3.41 ± 0.41
G		+negative		0.19 ± 0.09	0.20 ± 0.09
H		+positive	0.7 μM CQ_{ex}	1.08 ± 0.18	1.19 ± 0.11
I		+positive	12.5 μM CQ_{ex}	0.10 ± 0.02	0.08 ± 0.03
J		+positive	125 μM CQ_{ex}	0.24 ± 0.07	0.15 ± 0.05
K		+positive	1 μM VPL_{ex}	1.07 ± 0.12	1.08 ± 0.25
L		+positive	10 μM VPL_{ex}	1.09 ± 0.10	0.92 ± 0.21

[a](A) KCl pH 6.5 PL into KCl pH 6.5 buffer; (B) KCl pH 6.5 PL into KCl pH 7.5 buffer; (C) KCl pH 6.5 PL into KCl pH 8.5 buffer; (D) NaCl pH 6.5 PL into KCl pH 6.5 buffer; (E) KCl pH 6.5 PL into NaCl pH 6.5 buffer; (F) NaCl pH 6.5 PL into KCl pH 6.5 buffer with valinomycin; (G) KCl pH 6.5 PL into NaCl pH 6.5 buffer with valinomycin; (H) NaCl pH 6.5 PL into KCl pH 6.5 buffer with valinomycin and 0.7 μM CQ; (I) NaCl pH 6.5 PL into KCl pH 6.5 buffer with valinomycin and 12.5 μM CQ; (J) NaCl pH 6.5 PL into KCl pH 6.5 buffer with valinomycin and 125 μM CQ; (K) NaCl pH 6.5 PL into KCl pH 6.5 buffer with valinomycin and 1 μM VPL; (L) NaCl pH 6.5 PL into KCl pH 6.5 buffer with valinomycin and 10 μM VPL.

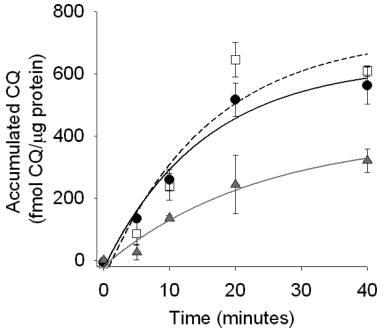

FIGURE 6: ISOV harboring the Dd2 isoform (▲) showed less ^{3}H-CQ uptake than HB3 (●), which were the same as control ISOV with no CRT. Amount of ^{3}H-CQ accumulated was measured from radioactivity measurements of filtered ISOV previously incubated with 100 nM ^{3}H-CQ for 0, 5, 10, 20, or 40 min. Single exponential fitting of data points gave rate constants for HB3 (solid black line, 0.0532 per second) and control (dashed black line, 0.0803 per second) ISOV, which were both greater than for Dd2 (solid gray line, 0.0431 per second).

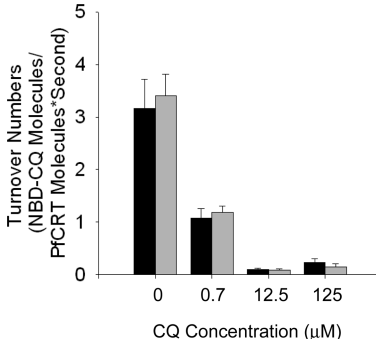

FIGURE 7: External CQ did not produce trans-stimulated NBD-CQ efflux for both HB3 (black bars) and Dd2 (gray bars) PL preloaded with 5 μM NBD-CQ. Instead, 0.7 μM or greater concentrations of CQ (12.5 or 125 μM) on the opposite side of the membrane decreased the rate of NBD-CQ efflux when $\Delta\Psi^+$ was present.

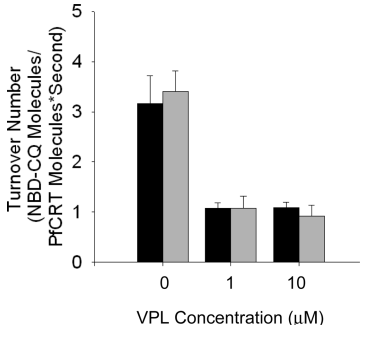

FIGURE 8: VPL inhibited HB3 (black bars) or Dd2 (solid bars) mediated NBD-CQ efflux. All turnover numbers were derived from 5 μM NBD-CQ preloaded PL in the presence of $\Delta\Psi^+$ and absence of ΔpH.

Finally, the effects of increasing external CQ and verapamil (VPL) concentrations on the efflux of 5 μM NBD-CQ from Dd2 and HB3 PL (Figures 7 and 8, respectively) were measured. Increasing external CQ concentration progressively slowed efflux of probe from both Dd2 and HB3 PL, and to a similar extent (Figure 7). External VPL concentration of 1 μM slowed efflux of 5 μM probe from both PL preparations by about 60%, and raising it to 10 μM did not further decrease probe flux (Figure 8).

DISCUSSION

Data in this paper and in the accompanying (*9*) provide the most direct evidence to date for PfCRT-mediated transport of quinoline compounds. NBD-CQ is a valid probe for CQ transport that behaves quite similar to CQ. Efflux assays using PL and ^{3}H-CQ via pointwise fast filtration methods are exceedingly tedious, have very poor kinetic resolution, and also have quite large variability due to hydrophobicity of the PL, the drug, and filters across which filtration must occur. So in spite of the structural differences between NBD-CQ and CQ, we have found transport studies with the former to be particularly informative. Nonetheless, some caution in interpretation of these data is warranted since addition of the fluorescent moiety does change CQ structure.

This study is the first to quantitatively compare quinoline transport at high kinetic resolution by purified reconstituted PfCRT-h isoforms as a function of ΔpH and $\Delta\Psi$. Since both ΔpH and $\Delta\Psi$ are high for the DV membrane (ΔpH is ~2 units (*24*) and $\Delta\Psi$ is expected to be > 70 mV and positive inside (*25*)), the

ability to quantify probe flux in the presence vs absence of these parameters for PL preparations is crucial. Through both equilibrium binding measurements (*7*) and photolabeling techniques (*10*), we previously defined direct binding of CQ to PfCRT protein. Competition for photolabeling efficiency revealed only small but important differences in CQ, QN, and mefloquine (MQ) binding for CQR vs CQS PfCRT-h isoforms (*10*). These data and others (*7*, *8*, *11*−*13*) further support PfCRT-catalyzed transport of quinoline drugs.

Data in this paper begin to more clearly quantify that transport. These data show that, in the absence of any ΔpH or ΔΨ, NBD-CQ flux mediated by either CQS (HB3) or CQR (Dd2) isoforms of PfCRT is low, corresponding to only 1 probe molecule per PfCRT molecule approximately every 5 s. In the presence of a 2 unit ΔpH, however, this increases to ∼2 probe molecules per PfCRT per second, and in the presence of a high $\Delta\Psi^{+}$, this increases further to >3 probe molecules per PfCRT per second. One other study has reported experiments with PfCRT PL, but this study did not examine efflux, rather it monitored gradient-driven *uptake* of ^{3}H-CQ *into* PL via filtration, without manipulating ΔpH or ΔΨ. Apparent turnover from 1 min time points in ref *26* yields 0.00002 CQ/PfCRT/second, which is 5 orders of magnitude lower than the turnover reported in the present study and far too low to account for reduced CQ uptake into CQR parasite DV (*9*). Presumably, if any drug transport via PfCRT was measured in ref *26*, this would suggest that PfCRT does not catalyze membrane transport at the same rate in both directions.

Regardless, perhaps consistent with similar CQ binding efficiencies for HB3 and Dd2 PfCRT isoforms (*7*, *10*), our turnover calculations suggest NBD-CQ efflux mediated by PfCRT is similar for HB3 vs Dd2 PL when either ΔpH or ΔΨ are fixed at similar values. At high ΔΨ, a small and reproducible increase is seen for Dd2 vs HB3 PL, although this was not found to be statistically significant with our current methods. Experiments with ^{3}H-CQ and ISOV did not suggest that HB3 PfCRT mediates increased influx relative to control but did show, similar to previous work (*7*, *11*), that the presence of Dd2 PfCRT reduced accumulation into the ISOV. Kinetic resolution of the ^{3}H-CQ data is poor so we are unable to unequivocally conclude whether accumulation into Dd2 ISOV proceeds with any significantly different rate constant relative to control or HB3 ISOV. However, accumulation of NBD-CQ into live intact iRBC (*9*) clearly showed a reduced rate constant for CQR parasites. Similar to earlier interpretation (*13*), the ATP dependence for this effect could be (in part) reflecting a DV pH, ΔpH, or ΔΨ dependence for PfCRT-mediated outward transport since these parameters are controlled by cytosolic ATP. The high ΔpH and ΔΨ dependence for PfCRT-mediated transport we observe in this paper is consistent with that idea.

It is important to note that no statistically significant efflux turnover differences were found for HB3 vs Dd2 PfCRT PL when ΔpH or ΔΨ were similar for the two PL preparations. It should also be noted then that the actual ΔpH across the DV membrane in live malaria parasites may be variable. While some groups conclude there is no significant difference in DV pH for CQR vs CQS parasites (*27*−*29*), other laboratories previously concluded DV pH for CQR vs CQS parasites differs (*24*, *30*, *11*). The different conclusions are likely related to variable sensitivity of the methods as discussed (*24*, *29*), since the pH differences are small (0.4−0.5 unit) and calculated using indirect fluorescence from a small organelle. If DV ΔpH are taken to be ∼1.5 units for HB3 and ∼2.0 units for Dd2 parasite (*24*), this would mean that the NBD-CQ turnover numbers reported for PL in this paper do not reflect the actual values that would occur for live parasites. Moreover, if these values for live parasite ΔpH are taken into consideration and if similar low DV ΔΨ exists for CQS and CQR parasites, then at 5 μM free NBD-CQ within the DV, HB3 PfCRT-mediated turnover would be 1.24 vs 1.96 for Dd2 (a net increase of ∼0.72 NBD-CQ/PfCRT/second for CQR parasites). If these differences in DV ΔpH for CQS vs CQR parasites are neglected, it might also be possible that higher ΔΨ for CQR DV membranes vs CQS drives a higher flux of CQ from the CQR DV. Therefore, we speculate that higher ΔpH and/or ΔΨ for CQR DV membranes, in some combination, promotes higher outward flux of CQ by mutant (CQR associated) PfCRT. Other studies have suggested CQ transport from the CQR DV occurs along with a significant H^{+} leak (*31*). This would also be explained by higher ΔpH and/or ΔΨ for CQR DV membranes, along with the data in this paper. Obviously, additional methods for measuring DV ΔΨ for live parasites within iRBC would help to further test key aspects of this model.

Unfortunately, no precise measure of PfCRT site density in the DV membrane is currently available. In the companion paper (*9*), we are able to quantify influx (at external concentrations that yield micromolar levels of probe within the DV in ∼15 min) to be ∼150 NBD-CQ per second per DV. But without precise values for PfCRT site density, DV membrane ΔΨ, or the exact percentage of intra-DV drug that is bound vs free when DV concentration approaches 5 μM (only free would be available for transport), we are unable to unequivocally conclude whether the PfCRT-mediated efflux we measure in this paper is sufficient to account entirely for the reduced accumulation rate constant noted for live CQR parasites. Morever, although no significant flux in the opposite direction is expected at the much lower extraproteliposomal [NBD-CQ] that occur during a PL efflux experiment, our PL have ∼75% of the PfCRT oriented one way and ∼25% the other (*10*), which might in theory slightly affect our turnover calculations at particularly high [NBD-CQ]. However, assuming (1) high ΔpH and ΔΨ for the DV as expected, (2) small differences in these parameters do exist for CQR vs CQS parasites as reported (*24*), and (3) a reasonable site density for PfCRT, then the efflux turnover differences we calculate in this paper would be compatible with PfCRT providing a significant contribution to reduced drug accumulation for CQR parasite DV relative to CQS.

However, our quantification of this meaningful but rather low turnover, along with data in ref *9*, leads us to suggest that PfCRT-mediated flux cannot be the only contributing factor to altered net accumulation of CQ vs time in CQR parasites. Data (*9*, *21*, *32*) clearly indicate a contribution that is due to altered binding. When exposed to drug for longer times at lower external dose such that the same total level of drug is accumulated vs CQS parasites, CQR parasites clearly bind progressively lower proportions of the drug, such that when zero trans efflux is initiated, more drug leaves the DV (Figure 5 in ref *9*). When external drug concentration is raised and incubation time shortened, CQS parasites bind less in ATP-dependent fashion (see also ref *20*) such that they then behave similar to CQR parasites in efflux assays (Figure 5 in ref *9*). Intra-DV drug binding behavior clearly differs for live CQS vs CQR parasites, and more extensive analysis of this altered binding is warranted. In the meantime, this leads us to suggest that the reduced rate constant for drug accumulation into CQR DV (*9*) is due to at least two effects:

increased ATP-dependent efflux via PfCRT (with ATP dependence manifested as ATP dependence for ΔΨ or ΔpH) and altered ATP-dependent drug binding.

Taking these data together then, we are able to distinguish between detailed models for altered CQ accumulation within live CQR parasite DV. The CQS parasite DV must accumulate CQ via at least two processes: passive influx (Figure 9A, "1") and some form(s) of ATP-dependent accumulation. The ATP-dependent accumulation could be either via an ATP-driven transporter (Figure 9A, "2") or via rate-limiting ATP-dependent binding to intra-DV heme targets (Figure 9A, "3"); regardless, it is compromised for CQR parasites whereas "1" must remain the same (see also Figure 4, panel E vs panel F, solid symbols, in ref *9*). To explain a reduced rate constant for accumulation into CQR DV, either "2" could be reduced (Figure 9B, denoted "2′"), or a new PfCRT-mediated efflux (Figure 9C, labeled "4") could kinetically compete with "1" and "2". In either scenario, "3" is altered (Figure 9B,C, denoted "3′") which further contributes to reduced accumulation. If "3" depends critically upon ATP and is rate limiting for net accumulation, then the process labeled "2" in Figure 9A perhaps reduces to process "3" (meaning, no "2" is necessary). We have eliminated the possibility that either PfMDR1 (see Table 2 in ref *9*) or CQS (HB3) isoform PfCRT (Figure 6, this paper) mediates a hypothesized "2′" (Figure 9B); thus we favor the model shown in Figure 9C. In this model, we predict time-, pH-, and volume-dependent binding of drug to various forms of heme is present within the DV as elaborated upon elsewhere (*21*, *33*−*35*). We envision that net reduced CQ accumulation for CQR DV is the sum of reduced binding to heme pools (Figure 9C; "3′") as well as increased electrochemically driven efflux via mutant PfCRT that is due to a higher electrochemical driving force for CQR DV (Figure 9C, "4"). Both of these processes are ATP dependent since cytosolic ATP controls intra-DV pH and other parameters central to the efficiency of heme to hemozoin conversion, and hence the availability of drug binding sites (*33*−*35*), and also controls the magnitude of DV membrane ΔpH and ΔΨ, which have large effects on drug efflux mediated by PfCRT.

Other proposals have included that PfCRT mediates CQ exchange or countertransport (*8*, *12*). Our data are not consistent with those models, as was also concluded in another study (*13*). One way to resolve whether PfCRT acts as a facilitative diffusion channel or as a transporter is to test for CQ countertransport. Only transporters are characterized by their ability to stimulate efflux when the same substrate also resides on the opposite side of the membrane. Hence, trans-efflux experiments were conducted wherein PfCRT PL preincubated with 5 μM NBD-CQ were diluted into different concentrations of unlabeled CQ such that the transmembrane ratios examined spanned those examined previously (*8*, *12*). The turnover numbers calculated for either HB3 (Figure 7, black bars) or Dd2 (Figure 7, gray bars) isoforms did not increase when 0.7 μM CQ was added externally. In fact, they were reduced and decreased even further when the CQ external concentrations were increased to 12.5 or 125 μM CQ. These findings do not agree with a recent study where trans-stimulated efflux was observed in both HB3 and Dd2 iRBC, with the latter giving higher initial efflux rates only when energy was present (*12*). Instead, data in this paper indicate that PfCRT behaves more as a channel-like transporter for positively charged CQ. Channels or channel-like molecules typically show decreased efflux rates when outward flow is blocked by the presence of external substrate and also exhibit linear rate vs substrate concentration plots (cf. Figure 5B). In contrast, rates of efflux for active carriers increase and eventually reach maximum when the concentration outside the cell is increased and typically show hyperbolic rate vs substrate concentration plots (*36*).

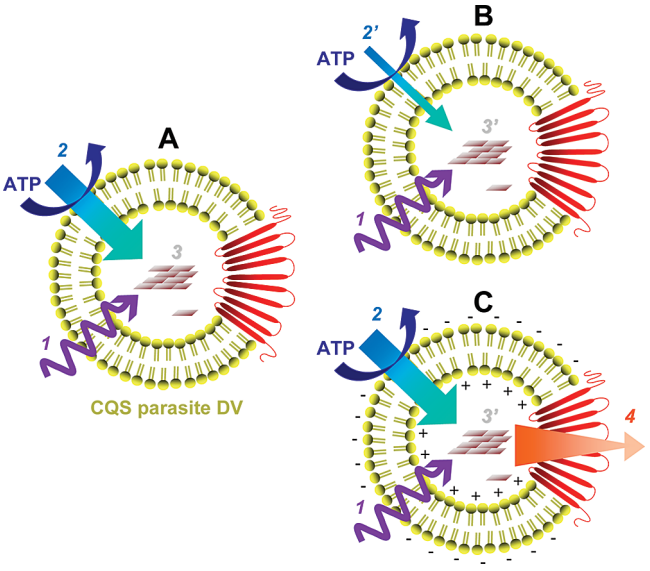

FIGURE 9: Proposed mechanism for altered CQ transport in CQR *P. falciparum*. (A) CQ transport in CQS parasites is regulated by passive influx (1), an ATP-dependent accumulation process (2), and binding to heme (3). (B) While similar passive influx is still present in CQR parasites, an ATP-dependent carrier becomes less active (2′) and heme binding is altered (3′) due to changes in DV pH and volume. These changes explain the reduced net accumulation of CQ associated with the CQR phenotype, including altered rate constant for influx shown in ref *9*. (C) Our data, however, support another model wherein CQR parasites harbor no change in ATP-dependent carrier (similar to 2, if it exists), altered binding (3′), and an additional ΔΨ-dependent efflux process (4) mediated by PfCRT.

In addition, the effect of VPL, a calcium-channel blocker that has been shown to reverse CQ resistance for some CQR *P. falciparum* (*37*), was investigated. In the channel model, VPL is speculated to work via positive charge which then blocks outward movement of protonated CQ through PfCRT (*7*, *13*, *37*). Alternatively, the transporter model proposes that VPL acts specifically by preventing the interconversion of CQR PfCRT to a state that allows the release of bound CQ (*12*). In this study, the presence of 1 or 10 μM VPL in the diluting buffer led to partially inhibited NBD-CQ efflux in Dd2 PL (Figure 8, gray bars). But unlike the results of other studies where VPL was found to inhibit CQ efflux only for Dd2 PfCRT (*12*, *13*, *37*), efflux was also inhibited in HB3 (Figure 8, black bars). Our initial VPL results therefore do not in and of themselves unequivocally distinguish channel vs carrier hypotheses; nonetheless, the bulk of our data are much more consistent with the former.

In conclusion, the kinetic and thermodynamic characterization of drug efflux from live parasite DV cannot be unequivocally quantified without controlling for unresolved time-dependent drug binding (Figure 5 in ref *9*), which is not well understood at present. Any contributions of PfCRT to live parasite DV efflux, as well as the effects of inhibitors and driving forces, can only be quantified with PL experiments at much higher kinetic resolution. Such work with a fluorescent CQ derivative that behaves similarly to CQ now clearly shows that PfCRT-mediated efflux is likely similar for CQS and CQR isoforms in the presence of similar electrochemical driving force but differs when these driving forces are larger for CQR DV membranes. This likely

contributes in a meaningful way to reduced cellular accumulation of drug for CQR parasites and, along with altered ATP-dependent drug binding within the cell, explains reduced net cellular drug accumulation for CQR parasites.

ACKNOWLEDGMENT

The authors thank Changan Xie for helpful discussions and Linda Amoah for creating the PfCRT-h constructs.

SUPPORTING INFORMATION AVAILABLE

One figure showing fluorescence changes for NBD-CQ-preloaded PL upon quenching by sodium dithionite at different time points. This material is available free of charge via the Internet at http://pubs.acs.org.

REFERENCES

1. Krogstad, D. J., Gluzman, I. Y., Kyle, D. E., Oduola, A. M. J., Martin, S. K., Milhous, W. K., and Schlesinger, P. H. (1987) Efflux of chloroquine from *Plasmodium falciparum*: mechanism of chloroquine resistance. *Science 238*, 1283–1285.
2. Fidock, D. A., Nomura, T., Talley, A. K., Cooper, R. A., Dzekunov, S. A., Ferdig, M. T., Ursos, L. M., Sidhu, A. B., Naude, B., Deitsch, K. W., Su, X. Z., Wootton, J. C., Roepe, P. D., and Wellems, T. E. (2000) Mutations in the *P. falciparum* digestive vacuole transmembrane protein PfCRT and evidence for their role in chloroquine resistance. *Mol. Cell 6*, 861–871.
3. Sidhu, A. B., Verdier-Pinard, D., and Fidock, D. A. (2002) Chloroquine resistance in *Plasmodium falciparum* malaria parasites conferred by *pfcrt* mutations. *Science 298*, 210–213.
4. Reed, M. B., Saliba, K. J., Caruana, S. R., Kirk, K., and Cowman, A. F. (2000) Pgh1 modulates sensitivity and resistance to multiple antimalarials in *Plasmodium falciparum*. *Nature 403*, 906–909.
5. Sidhu, A. B., Valderramos, S. G., and Fidock, D. A. (2005) *pfmdr1* mutations contribute to quinine resistance and enhance mefloquine and artemisinin sensitivity in *Plasmodium falciparum*. *Mol. Microbiol. 57*, 913–926.
6. Sanchez, C. P., Rotmann, A., Stein, W. D., and Lanzer, M. (2008) Polymorphisms within PfMDR1 alter the substrate specificity for anti-malarial drugs in *Plasmodium falciparum*. *Mol. Microbiol. 70*, 786–798.
7. Zhang, H., Paguio, M., and Roepe, P. D. (2004) The antimalarial drug resistance protein *Plasmodium falciparum* chloroquine resistance transporter binds chloroquine. *Biochemistry 43*, 8290–8296.
8. Sanchez, C. P., Stein, W., and Lanzer, M. (2003) Trans stimulation provides evidence for a drug efflux carrier as the mechanism of chloroquine resistance in *Plasmodium falciparum*. *Biochemistry 42*, 9383–9394.
9. Cabrera, M., Natarajan, J., Paguio, M. F., Wolf, C., Urbach, J. S., and Roepe, P. D. (2009) Chloroquine transport in *Plasmodium falciparum*. 1. Influx and efflux kinetics for live trophozoite parasites using a novel fluorescent chloroquine probe, *Biochemistry* (DOI 10.1021/bi901034r).
10. Lekostaj, J. K., Natarajan, J. K., Paguio, M. F., Wolf, C., and Roepe, P. D. (2008) Photoaffinity labeling of the *Plasmodium falciparum* chloroquine resistance transporter with a novel perfluorophenylazido chloroquine. *Biochemistry 47*, 10394–10406.
11. Naude, B., Brzostowski, J. A., Kimmel, A. R., and Wellems, T. E. (2005) *Dictyostelium discoideum* expresses a malaria chloroquine resistance mechanism upon transfection with mutant, but not wild-type, *Plasmodium falciparum* transporter PfCRT. *J. Biol. Chem. 280*, 25596–25603.
12. Sanchez, C. P., Rohrbach, P., McLean, J. E., Fidock, D. A., Stein, W. D., and Lanzer, M. (2007) Differences in trans-stimulated chloroquine efflux kinetics are linked to PfCRT in *Plasmodium falciparum*. *Mol. Microbiol. 64*, 407–420.
13. Bray, P. G., Mungthin, M., Hastings, I. M., Biagini, G. A., Saidu, D. K., Lakshmanan, V., Johnson, D. J., Hughes, R. H., Stocks, P. A., O'Neill, P. M., Fidock, D. A., Warhurst, D. C., and Ward, S. A. (2006) PfCRT and the trans-vacuolar proton electrochemical gradient: regulating the access of chloroquine to ferriprotoporphyrin IX. *Mol. Microbiol. 62*, 238–251.
14. Gligorijevic, B., Bennett, T., McAllister, R., Urbach, J. S., and Roepe, P. D. (2006) Spinning disk confocal microscopy of live, intraerythrocytic malarial parasites. 2. Altered vacuolar volume regulation in drug resistant malaria. *Biochemistry 45*, 12411–12423.
15. Zhang, H., Howard, E. M., and Roepe, P. D. (2002) Analysis of the antimalarial drug resistance protein Pfcrt expressed in yeast. *J. Biol. Chem. 277*, 49767–49775.
16. Delhez, J., Dufour, J.-P., Thines, D., and Goffeau, A. (1977) Comparison of the properties of plasma membrane-bound and mitochondria-bound ATPases in the yeast *Schizosaccharomyces pombe*. *Eur. J. Biochem. 79*, 319–328.
17. Howard, E. M., and Roepe, P. D. (2003) Purified human MDR 1 modulates membrane potential in reconstituted proteoliposomes. *Biochemistry 42*, 3544–3555.
18. Amoah, L. E., Lekostaj, J. K., and Roepe, P. D. (2007) Heterologous expression and ATPase activity of mutant versus wild type PfMDR1 protein. *Biochemistry 46*, 6060–6073.
19. Menendez, A., Larsson, C., and Ugalde, U. (1995) Purification of functionally sealed cytoplasmic side-out plasma membrane vesicles from *Saccharomyces cerevisiae*. *Anal. Biochem. 230*, 308–314.
20. Fitch, C. D. (1969) Chloroquine resistance in malaria: A deficiency of chloroquine binding. *Proc. Natl. Acad. Sci. U.S.A. 64*, 1181–1187.
21. Bray, P. G., Mungthin, M., Ridley, R. G., and Ward, S. A. (1998) Access to hematin: the basis of chloroquine resistance. *Mol. Pharmacol. 54*, 170–179.
22. McIntyre, J. C., and Sleight, R. G. (1991) Fluorescence assay for phospholipid membrane asymmetry. *Biochemistry 30*, 11819–11827.
23. Ohnishi, M., and Urry, D. W. (1970) Solution conformation of valinomycin-potassium ion Complex. *Science 168*, 1091–1092.
24. Bennett, T. N., Kosar, A. D., Ursos, L. M. B., Dzekunov, S., Sidhu, A. B. S., Fidock, D. A., and Roepe, P. D. (2004) Drug resistance-associated pfCRT mutations confer decreased *Plasmodium falciparum* digestive vacuolar pH. *Mol. Biochem. Parasitol. 133*, 99–114.
25. Yabe, I., Horiuchi, K., Nakahara, K., Hiyama, T., Yamanaka, T., Wang, P. C., Toda, K., Hirata, A., Ohsumi, Y., Hirata, R., Anraku, Y., and Kusaka, I. (1999) Patch clamp studies on V-type ATPase of vacuolar membrane of haploid *Saccharomyces cerevisiae*. Preparation and utilization of a giant cell containing a giant vacuole. *J. Biol. Chem. 274*, 34903–34910.
26. Tan, W., Gou, D. M., Tai, E., Zhao, Y. Z., and Chow, L. M. (2006) Functional reconstitution of purified chloroquine resistance membrane transporter expressed in yeast. *Arch. Biochem. Biophys. 452*, 119–128.
27. Hayward, R., Saliba, K. J., and Kirk, K. (2006) The pH of the digestive vacuole of *Plasmodium falciparum* is not associated with chloroquine resistance. *J. Cell Sci. 119*, 1016–1025.
28. Kuhn, Y., Rohrbach, P., and Lanzer, M. (2007) Quantitative pH measurements in *Plasmodium falciparum*-infected erythrocytes using pHluorin. *Cell. Microbiol. 9*, 1004–1013.
29. Klonis, N., Tan, O., Jackson, K., Goldberg, D., Klemba, M., and Tilley, L. (2007) Evaluation of pH during cytostomal endocytosis and vacuolar catabolism of haemoglobin in *Plasmodium falciparum*. *Biochem. J. 407*, 343–354.
30. Reeves, D. C., Liebelt, D. A., Lakshmanan, V., Roepe, P. D., Fidock, D. A., and Akabas, M. H. (2006) Chloroquine-resistant isoforms of the *Plasmodium falciparum* chloroquine resistance transporter acidify lysosomal pH in HEK293 cells more than chloroquine-sensitive isoforms. *Mol. Biochem. Parasitol. 150*, 288–299.
31. Lehane, A. M., and Kirk, K. (2008) Chloroquine resistance-conferring mutations in pfcrt give rise to a chloroquine-associated H^+ leak from the malaria parasite's digestive vacuole. *Antimicrob. Agents Chemother. 52*, 4374–4380.
32. Bray, P. G., Janneh, O., Raynes, K. J., Mungthin, M., Ginsburg, H., and Ward, S. A. (1999) Cellular uptake of chloroquine is dependent on binding to ferriprotoporphyrin IX and is independent of NHE activity in *Plasmodium falciparum*. *J. Cell Biol. 145*, 363–376.
33. Leed, A., Dubay, K., Ursos, L. M., Sears, D., de Dios, A. C., and Roepe, P. D. (2002) Solution structures of antimalarial drug-heme complexes. *Biochemistry 41*, 10245–10255.
34. Casabianca, L. B., An, D., Natarajan, J. K., Alumasa, J. N., Roepe, P. D., Wolf, C., and de Dios, A. C. (2008) Quinine and chloroquine differentially perturb heme monomer-dimer equilibrium. *Inorg. Chem. 47*, 6077–6081.
35. Casabianca, L. B., Kallgren, J. B., Natarajan, J. K., Alumasa, J. N., Roepe, P. D., Wolf, C., and de Dios, A. C. (2009) Antimalarial drugs and heme in detergent micelles: an NMR study. *J. Inorg. Biochem. 103*, 745–748.
36. Stein, W. D. (1990) Channels, Carriers, and Pumps: An Introduction to Membrane Transport , Academic Press, San Diego, CA.
37. Martin, S. K., Oduola, A. M., and Milhous, W. K. (1987) Reversal of chloroquine resistance in *Plasmodium falciparum* by verapamil. *Science 235*, 899–901.